Available online at www.sciencedirect.com
SCIENCE DIRECT®
ELSEVIER
Applied Surface Science 212–213 (2003) 654–660
applied surface science
www.elsevier.com/locate/apsusc

Optical properties of polycrystalline and epitaxial anatase and rutile TiO_2 thin films by rf magnetron sputtering

S. Tanemura[a,*], L. Miao[a], P. Jin[b], K. Kaneko[c], A. Terai[d], N. Nabatova-Gabain[d]

[a]*Department of Environmental Technology and Urban Planning, Nagoya Institute of Technology, Gokisho-cho, Showa-ku, Nagoya 466-8555, Japan*
[b]*Institute of Structural and Engineering Materials, National Institute of Advanced Industrial Science and Technology (AIST), Moriyama-ku, Nagoya 463-8560, Japan*
[c]*Department of Materials Science and Engineering HVEM Laboratory, Kyushu University, Higasi-ku, Hakozaki 6-10-1, Fukuoka 812-8581, Japan*
[d]*Horiba Jobin-Yvon Co. Ltd., 1-7-8 Higashi-kanda, Chiyoda-ku, Tokyo 101-0031, Japan*

Abstract

We analyzed successfully the refractive index n, extinction coefficient k, and optical band gap E_g of the fabricated polycrystalline and epitaxial TiO_2 films of rutile and anatase films by spectroscopic ellipsometry (SE). The provided samples were prepared by rf magnetron sputtering of TiO_2 target with Ar gas plasma under a variety of sputtering parameters such as total pressure, Ar gas flow rate, O_2 gas flow rate, applied sputtering power, substrate temperature and substrate materials. The covered wavelength for SE was from 0.75 to 5 eV (1653–248 nm in wavelength). As the conclusion, the films show higher values of refractive indices than the previously reported ones by other authors. Optical band gaps extrapolated by Tauc plot using the obtained extinction coefficient again show higher values than the known bulk data.

PACS: 78.20; 07.60.R; 78.20.c; 71.20

Keywords: SE; TiO_2; Thin film; Complex refractive index; Optical band gap

1. Introduction

In recent years, titanium dioxide (TiO_2) thin films, of which most commonly used polymorphs are anatase and/or rutile, have attracted a lot of interests for its wide uses in photovoltaic devices [1–3], photocatalysts [4], waveguiding [5], semiconductor [6,7], storage capacitors in dynamic random access memories (DRAM) [8] and others. Optical properties, such as complex refractive indices ($n - ik$, where i is the unit of imaginary) for a certain range of wavelength between ultra violet and near infrared, and optical band gap values E_g, are becoming quite important criteria for the selection of the applications of the fabricated films.

We have already reported the success of the simultaneous fabrication of epitaxial anatase film on the substrate of single crystal $SrTiO_3$ and/or epitaxial rutile film on that of sapphire single crystal by rf magnetron sputtering under optimization of substrate temperature, total pressure, oxygen additives, and applied rf power [9]. Moreover, polycrystalline films of rutile and anatase were formed on Si substrate again by rf sputtering under

* Corresponding author. Tel.: +81-52-735-5024; fax: +81-52-735-5024.
E-mail address: saktane@system.nitech.ac.jp (S. Tanemura).

0169-4332/03/$ – see front matter
doi:10.1016/S0169-4332(03)00015-1

the similar conditions of substrate temperature, total pressure, oxygen additives, and applied rf power to epitaxial ones [10,11]. In the previous reports, comparison of the optical properties was briefly summarized.

In this report, we described the details of the study on spectroscopic ellipsometry (SE) to obtain the dispersion relation of complex refractive index from 0.75 to 5 eV (1653–248 nm in wavelength) for both the polycrystalline and the epitaxial TiO_2 thin films with anatase and rutile structure of which fabrication was described in the cited previous reports [9–11]. Optical band gaps E_g for the respective films extrapolated by Tauc plot using the obtained extinction coefficient are discussed. The evaluated optical properties are compared with those of the recent TiO_2 films [12,13] and bulk ones [14,15], and the reasons accounting for these properties differences are inferred.

2. Experimental

SE measurement was performed by the instrument with piezo elastic modulator (UVISE, Horiba Jobin-Yvon Co. Ltd., Tokyo) in the spectral range of 248–1653 nm [16,17]. The angle of incidence was set at a certain angle between 60 and 70° in arc to maximize an ellipsometric parameter ψ which is amplitude ratio between reflected s polarized component and that of p component. One of the technical advantage of the used instrument is assurance of measurement accuracy of an ellipsometric parameter Δ (phase difference between reflected s polarized component and that of p component) in the point of detecting $\sin\Delta$ alternatively $\cos\Delta$ particularly for a small angle of Δ.

As the complex refractive indices of the substrates are required in some cases to analyze optimal refractive index of the thin film, complex refractive indices of $SrTiO_3$, sapphire, and naturally oxidized Si single crystal were obtained in prior to the measurement of films and the necessary data being stored in the computer data base for further film analysis.

3. Details of analysis

3.1. Surface layer

First of all, we tested whether we could neglect the extremely thin surface layer for the provided samples. Consequently, a thin surface layer should be required to minimize χ^2 which is usually defined as the square of the residue between measured set of $(\psi_M(\lambda), \Delta_M(\lambda))$, where λ means wavelength, and theoretically calculated set of $(\psi_T(\lambda), \Delta_T(\lambda))$. Hereafter, we treat the present films as double layered configuration named as a surface layer and a primary layer. The optimized surface layer thickness, the applied optical function for the layer, and the values of the optimized parameters of the function are summarized in Table 1 for the provided samples.

In the case of epitaxial anatase, roughness model is suggested to be favorable, and consequently a classical Bruggeman effective medium theory is applied under the optimized volume fractions of both void and medium (TiO_2) as shown in Table 1. Moreover, the complex refractive index of the medium is assumed to the same with the primary layer.

In other samples, the slightly modified F&B optical function formula [18] developed for both crystalline semiconductor and dielectrics is applied. The modification is made by the following proposed J&M optical function formula [19] to solve the errors appeared on original F&B formula. This improvement assures that the parameterization fits the data better than F&B formula for thin film samples. For the explanation of the fitting parameters in Table 1, the employed dispersion function of extinction coefficient k and refractive index n as photon energy E are written as follows [17]:

$$k(E) = \left[\sum_{i=1}^{q} \frac{A_i}{E^2 - B_i E + C_i}\right](E - E_g)^2 \quad \text{for} \quad E > E_g \tag{1a}$$

$$k(E) = 0 \quad \text{for} \quad E \le E_g \tag{1b}$$

where E_g is energy-band gap and/or absorption edge. A_i, B_i, C_i and E_g are treated as fitting parameters. Then n is given by

$$n(E) = n(\infty) + \sum_{i=1}^{q} \frac{B_{0i}E + C_{0i}}{E^2 - B_i E + C_i} \tag{2}$$

where $n(\infty)$ is related with dielectric function ε by $(\varepsilon(\infty))^{1/2}$ as $E \to \infty$, and B_{0i} and C_{0i} are rewritten by

$$B_{0i} = \frac{A_i}{Q_i}\left[-\frac{B_i^2}{2} + E_g B_i E_g^2 + C_i\right] \tag{3}$$

Table 1
Summary of the optimized parameters of the surface layer

Film configuration	Anatase		Rutile	
	Epitaxial	Polycrystal	Epitaxial	Polycrystal
Surface layer thickness (nm)	4.37	7.40	4.81	12.63
Applied optical function	Bruggeman theory	Double terms of F&B formula[a]	Single terms of F&B formula[a]	Double terms of F&B formula[a]
Optimized values of the parameters	(1) Volume fraction	[b]	[b]	[b]
	Void (air): 58.56%	E_∞: 2.811	E_∞: 0.919	E_∞: 3.534
	TiO_2: 41.44%	E_g: 0.845 A_1: 0.011	E_g: 1.969 A: 0.261	E_g: 1.361 A_1: 0.015
	(2) n and k: optimized values for the primary layer	B_1: 8.362	B: 8.717	B_1: 8.029
		C_1: 17.640 A_2: 0.016 B_2: 10.062 C_2: 25.558	C: 19.724	C_1: 16.214 A_2: 0.107 B_2: 9.229 C_2: 22.153

[a] See Eqs. (1a) and (1b).
[b] Listed values being different from those optimized for primary layer.

$$C_{0i} = \frac{A_i}{Q_i}\left[(E_g^2 + C_i)\frac{B_i}{2} - 2E_g C_i\right] \quad (4)$$

where

$$Q_i = \tfrac{1}{2}(4C_i - B_i^2)^{1/2} \quad (5)$$

3.2. Primary layer

For the primary layer, above described F&B functions are applied to all samples. The optimized thickness of main layer and values of parameters as well as minimized χ^2 value for each sample are summarized in Table 2. The numbers of the term required in the F&B formula are also shown in the second line of Table 2. Except the epitaxial anatase case, required numbers of terms for a surface layer and a primary one are identical with each other. The total film thickness, which is arithmetically summation of the thickness of surface and primary, agree satisfactorily with experimentally estimated values during film fabrication.

Table 2
Summary of the optimized parameters of the primary layer

	Anatase		Rutile	
	Epitaxial	Polycrystal	Epitaxial	Polycrystal
Primary layer thickness (nm)	152.3	156.9	136.9	131.34
Applied optical function	Double terms	Double terms	Single term	Double terms
Optimized values of the parameters	E_∞: 4.623 E_g: 3.339 A_1: 0.234 B_1: 9.507 C_1: 22.900 A_2: 0.138 B_2: 7.758 C_2: 15.097	E_∞: 4.952 E_g: 3.126 A_1: 0.145 B_1: 7.878 C_1: 15.653 A_2: 0.107 B_2: 9.389 C_2: 22.241	E_∞: 5.389 E_g: 2.842 A: 0.223 B: 8.151 C: 16.774	E_∞: 5.583 E_g: 3.032 A_1: 0.258 B_1: 7.769 C_1: 15.287 A_2: 0.065 B_2: 9.128 C_2: 20.964
Minimum value χ^2	0.387	0.89	11.87	1.12

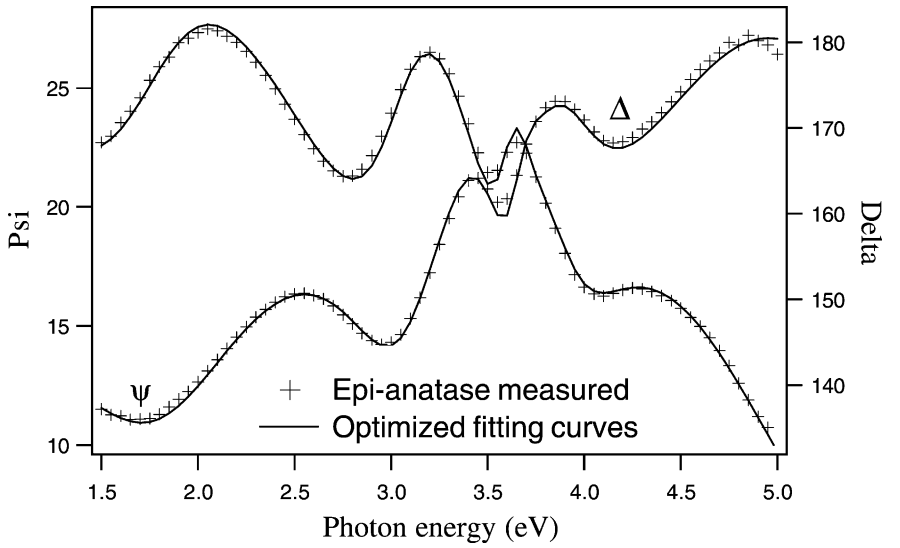

Fig. 1. Comparison between measured ellipsometric parameters and theoretical ones by optimized parameterization for epitaxial anatase.

Examples of the fitting of the measured ellipsometric parameters $\psi(+)$ and $\Delta(+)$ to theoretically calculated ones by optimized parameterization ψ(line) and Δ(line) are given in Figs. 1 and 2 for epitaxial anatase and epitaxial rutile films, respectively. The former stands for the case of minimum χ^2 value and the later for the maximum value.

It is worthwhile to describe the reason for extremely large χ^2 in the case of epitaxial rutile, that is, the back reflection of sapphire substrate which caused ripples

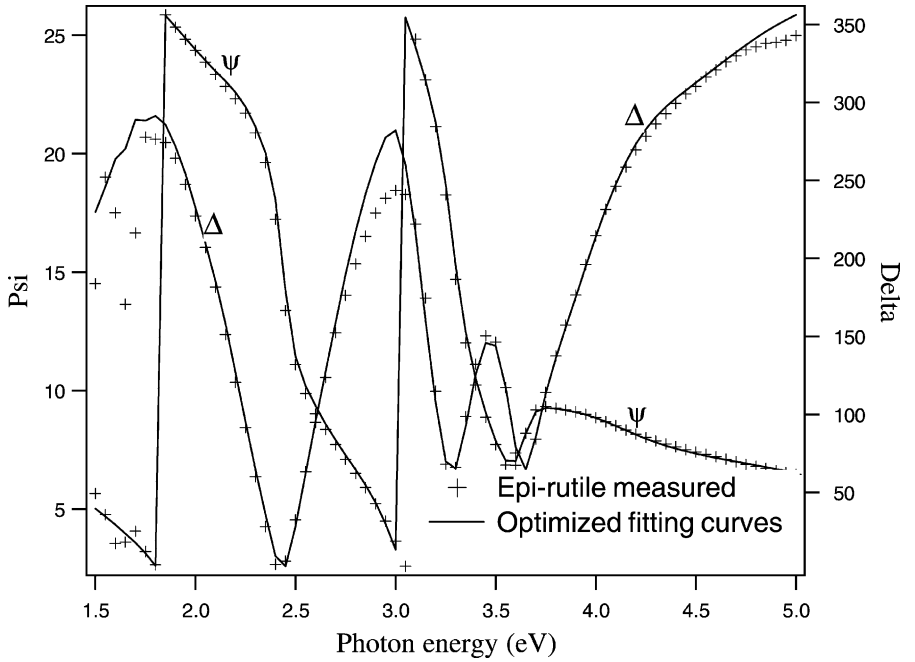

Fig. 2. Comparison between measured ellipsometric parameters and theoretical ones by optimized parameterization for epitaxial rutile.

of n and k throughout the designated wavelength. One can observe the apparent discrepancy of Δ for $E < 1.8$ eV, 2.8 eV $< E < 3.1$ eV, and $E > 4.8$ eV, and that of ψ for $E < 1.8$ eV, while it is consistency in the other photon energy range.

4. Results and discussions

The refractive index n and extinction coefficient k of both epitaxial and polycrystalline anatase films are given, respectively, in Fig. 3 as a function of photon energy. Those for both epitaxial and polycrystalline rutile films are shown, respectively, in Fig. 4. The obtained refractive indices (n) in the designated wavelength range show higher values than the values cited in the recent articles [12,13]. The representative value at 500 nm wavelength, the maximum value from 400 to 800 nm and the maximum value from 248 to 1653 nm are given in Table 3. The higher refractive indices give an evidence for the fine crystalline of the fabricated films.

Comparing dispersion relation of refractive indices n of epitaxial films with that of polycrystalline ones, we clearly observe the followings: (1) distinct two humps in high-energy region after exceeding band gap, which is usually observed in semi-conducting Ga compounds and In ones, in epitaxial anatase; and (2) steep peak in epitaxial rutile. The reasons are due to densely fine crystallinity of epitaxial anatase and rutile films. The dispersion relation of complex refractive index of rutile film is quite similar to that of the bulk material in the textbook [20].

The optical band gap E_g of the polycrystalline and epitaxial TiO_2 films was determined using the extinction coefficient k from the following Tauc expression under ad hoc assumption of predomination of indirect allowed transition mode [21]:

$$E - E_g = \left\{ \left(\frac{4\pi\kappa}{\lambda} \right) \frac{h\upsilon}{B} \right\}^{1/2} \tag{6}$$

where E is the photon energy ($\equiv h\upsilon$), B the constant, $h\upsilon$ the photon energy, $4\pi\kappa/\lambda$ the absorption coefficient at wavelength $\lambda(\alpha)$, and κ is the extinction coefficient. Since the right hand side values of Eq. (6) for respective sample is asymptotically approximated by the linear relation with photon energy particularly near absorption edge, a band gap value is given as the intercept of the photon energy axis and the linear line. This confirms the previous ad hoc assumption that

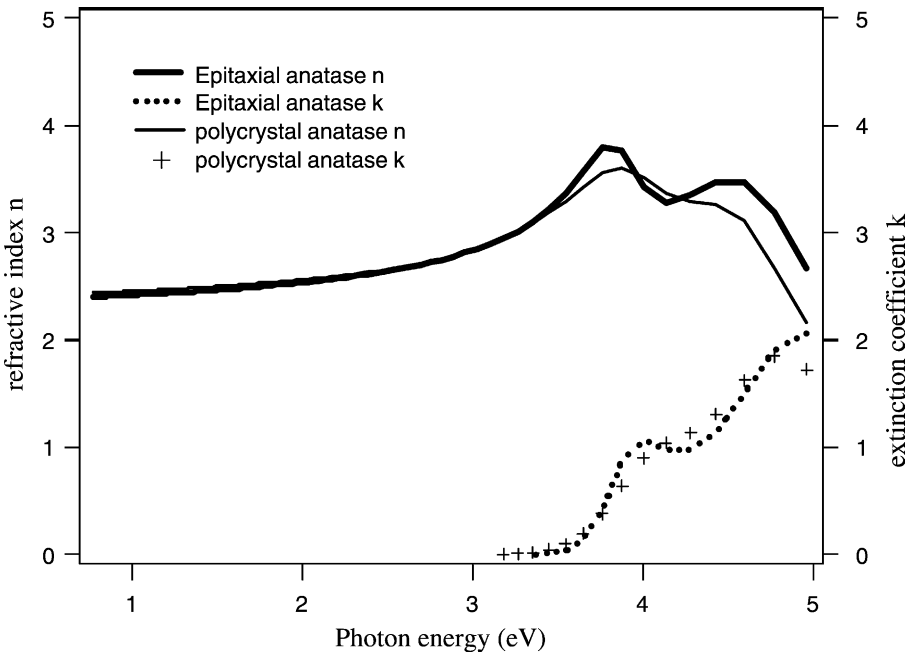

Fig. 3. Photon energy dependent refractive indices of both polycrystalline and epitaxial anatase films.

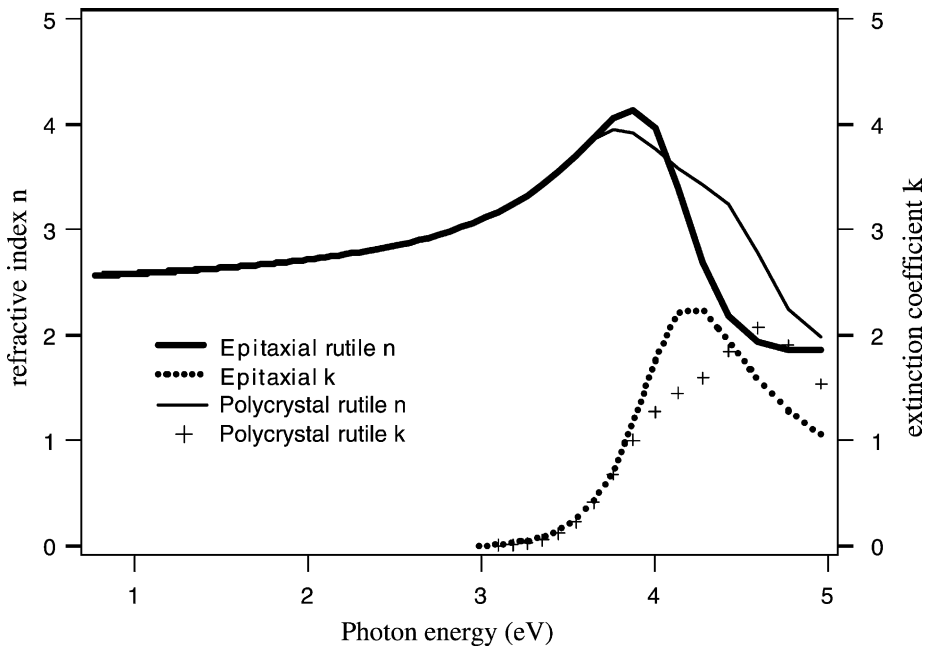

Fig. 4. Photon energy dependent refractive indices of both polycrystalline and epitaxial rutile films.

TiO_2 has a direct forbidden gap, which is also degenerated with an indirect allowed transition, the indirect allowed transition dominates in the optical absorption just above the absorption edge due to the weak strength of the direct forbidden transition [22,23]. It is noted that the optical band gap obtained by Tauc plot always different from that in F&B formula.

The plotted band gap values of anatase and rutile thin films are listed in Table 4. All values are larger than those of bulk [14,15] by about 10%. There are two possible reasons for a large band gap value of the film: (1) presumably due to an axial strain effect from lattice deformation as has been pointed out for ZnO films [24]; and (2) probably due to a change in the density of

Table 3
Values of refractive index n at the designated wavelength

	Rutile		Anatase	
	Polycrystalline	Epitaxial	Polycrystalline	Epitaxial
n at 500 nm	2.849	2.843	2.657	2.637
Maximum n at 400–800 nm	3.182 (400)	3.173 (400)	2.898 (400)	2.892 (400)
Maximum n at 250–1600 nm	3.952 (330)	4.142 (320)	3.605 (320)	3.79 (330)

Table 4
Band gap of the anatase and rutile films by Tauc plot in comparison to the bulk

Structure	Polycrystalline rutile film	Polycrystalline anatase film	Epitaxial rutile film	Epitaxial anatase film	Bulk rutile	Bulk anatase
Band gap E_g (eV)	3.34	3.39	3.37	3.51	3.03	3.20

semiconductor carriers. Which of the above is the dominant requires further study.

5. Conclusions

We analyzed successfully the refractive index n, extinction coefficient k, and optical band gap E_g of the fabricated polycrystalline and epitaxial TiO_2 films of rutile and anatase structure by SE, respectively. The double layered film configuration and the use of the modified F&B formula as the optical functions of n and k resulted in the best fitting of the measured ellipsometric parameters ψ and Δ to the theoretical ones.

The obtained real part of refractive indices (n) in the designated wavelength range for all provided samples show higher values than the values cited in the recent articles partly due to the fine crystallinity of the present samples. Comparing the dispersion relation of refractive index n of epitaxial film with polycrystal one, distinct two humps in high-energy region after exceeding band gap in epitaxial anatase and steep peak in epitaxial rutile are characteristic. This indicates fine crystallinity of the fabricated epitaxial films.

Optical band gaps E_g extrapolated using Tauc plot were about 10% larger than the bulk. Reasons for a large band gap value of the film is presumably due to an axial strain effect and probably further to a change in the density of semiconductor carriers.

References

[1] K. Kalayanasundaram, M. Grazel, E. Pelizzetti, Coord. Chem. Rev. 69 (1969) 57.
[2] B.A. Perkinson, M.T. Spitlet, Electrochem. Acta 37 (1992) 943.
[3] A. Haggfeldt, U. Bjorksten, S.-E. Lindquist, Solar Energy Mater. Solar Cells 27 (1992) 293.
[4] S. Tokita, N. Tanaka, H. Saitoh, Jpn. J. Appl. Phys. 2 39 (2000) L169.
[5] A. Bahtat, M. Bouderbala, M. Bahtat, M. Bouazaoui, J. Mugnier, M. Druetta, Thin Solid Films 323 (1998) 59.
[6] H. Fukuda, S. Namioka, M. Miura, Y. Ishikawa, M. Yoshino, S. Nomura, Jpn. J. Appl. Phys. 1 38 (1999) 6034.
[7] M.B. Lee, M. Kawasaki, M. Yoshimoto, B.K. Moon, Jpn. J. Appl. Phys. 1 34 (1995) 808.
[8] J.Y. Gan, Y.C. Chang, T.B. Wu, Appl. Phys. Lett. 72 (1998) 332.
[9] L. Miao, P. Jin, K. Kaneko, A. Terai, N. Nabatova-Gabain, S. Tanemura, Jpn. J. Cryst. Growth, 2003, submitted.
[10] L. Miao, P. Jin, K. Kaneko, S. Tanemura, J. Nano Tech., 2002, in press.
[11] L. Miao, S. Tanemura, P. Jin, K. Kaneko, A. Terai, N. Nabotova-Gabin, Appl. Surf. Sci., 2003, in press.
[12] C.C. Ting, S.Y. Chen, J. Appl. Phys. 88 (8) (2000) 4682.
[13] M.H. Suhail, G. Mohan Rao, S. Mohan, J. Appl. Phys. 71 (3) (1992) 1421.
[14] D.C. Cronemeyer, Phys. Rev. B 87 (1952) 876.
[15] H. Tang, F. Levy, H. Berger, P.E. Schmid, Phys. Rev. B 52 (1995) 7771.
[16] B. Drevillon, J.Y. Parney, M. Stchakovsky, SPIE 1188 (1989) 174.
[17] N. Nabatova-Gabain, Application of Spectro Scopic Ellipsometry for Material Characterization, Horiba Jobin-Yvon Co. Ltd., Tokyo, 2002, in press.
[18] A.R. Forouhi, I. Bloomer, Phys. Rev. B 38 (1988) 1865.
[19] G.E. Jellison Jr., F.A. Modie, Appl. Phys. Lett. 69 (1996) 371.
[20] M.W. Ribalski, Hand Book of Optical Constant of Solids, Academic Press, New York, 1985, pp. 795–804.
[21] J. Tauc, Optical Properties of Solids, North-Holland, Amsterdam, p. 303.
[22] N. Daude, C. Gout, C. Jouanin, Phys. Rev. B 15 (1977) 3229.
[23] K.M. Glassford, J.R. Chelikowsky, Phys. Rev. B 46 (1992) 1284.
[24] H.C. Ong, A.X.E. Zhu, Appl. Phys. Lett. 80 (2002) 941.